



Integrated workflow to investigate the fracture interference effect on shale well performance

Ahmed Farid Ibrahim^{1,2}

Received: 31 January 2022 / Accepted: 2 May 2022 / Published online: 7 June 2022
© The Author(s) 2022

Abstract

Horizontal drilling and multistage hydraulic fracturing applied in shale formations over the past decade. The operators are trying even closer cluster spacing to increase the initial rate, but it is at the expense of higher operation costs and complexity. This study presents an integrated workflow to investigate the effect of cluster interference on well performance. Analytical rate transient analysis (RTA) was combined with reservoir numerical simulation to calculate the effective fracture surface area (A_{Ce}) for hydrocarbon production. A proxy model was built to estimate the effective to actual stimulated fracture area ratio as a function of completion and reservoir parameters. The integrated workflow was applied to actual field data for two shale gas wells. An economic study was conducted to investigate the optimum spacing based on the well profitability. The well with a higher stage number and tighter cluster spacing had high cluster interference with a low A_{Ce}/A_{Ca} ratio. The well will drain the production area near the wellbore faster with a high initial production rate but with high production declining rate. Increasing the cluster spacing, with the same injected proppant volume, showed an increase in the A_{Ce}/A_{Ca} ratio, and a decrease in cluster interference. A lower initial rate was observed with a low production declining rate. Economic study showed optimum spacing of 60 ft based on the formation properties, capital cost, and gas price. As the interest rate, gas prices, and increases or low capital costs, the optimum completion tends to be with the tighter spacing to accelerate the production.

Keywords Cluster spacing · Interference · Shale formation

List of symbols

A_{Ce}	Effective fracture surface area, ft ²
A_{Ca}	Actual fracture surface, ft ²
AI	Artificial intelligence
RF	Random forest
RTA	Rate transient analysis
H_f	Fracture height, ft
X_f	Fracture half-length, ft
N_f	Number of fractures
p_{wf}	Bottom-hole pressure, psi
$m_{(p_{wf})}$	Pseudopressure
ϕ	Formation porosity
μ	Gas viscosity, cp

c_t	Total compressibility, psi ⁻¹
PTA	Pressure transient analysis
T	Temperature, R
RF	Random forest
NPV	Net present value, \$
SRV	Stimulated reservoir volume, ft ³
Super	Linear superposition time
n	Number of the time step at which Super- t is calculated
j	Time step counter from 0 to n to calculate Super- t
p_i	Initial reservoir pressure, psi
k	Formation permeability, md

✉ Ahmed Farid Ibrahim
ahmed.ibrahim@kfupm.edu.sa

¹ Department of Petroleum Engineering and Geosciences, King Fahd University of Petroleum & Minerals, Dhahran 31261, Saudi Arabia

² Center for Integrative Petroleum Research, King Fahd University of Petroleum & Minerals, Dhahran 31261, Saudi Arabia

Introduction

In shale-gas reservoirs, ultralow-permeability matrix is not capable to flow fluid at a feasible rate and delivering an acceptable drainage volume. Horizontal drilling with multistage fracture completion has turned out to be the key stimulation technology for the development of shale plays (Wiley et al. 2004; King 2010; Beckwith 2011). Wells are

to accomplish a series of fracturing processes, with a high injection rate, large fracturing slurry volume, and low proppant concentration, during the multistage design (Seale et al. 2006; Sen et al. 2018; Kolawole et al. 2019; Singh et al. 2019). Different hydraulic fracturing fluid systems that can be used in the fracturing process include cross-linked high viscosity systems, foam-based fluids, and slickwater (Al-Muntasheri et al. 2009; Emrani et al. 2017; Ibrahim et al. 2018).

The economic feasibility and production improvement of an oil and gas well largely depend on the efficiency of hydraulically generated fractures (Ashraf et al. 2020; Jiang et al. 2021; Ullah et al. 2022). Under the current low gas price, it is mainly necessary and critical to generate the maximum number of active fractures along the horizontal wellbore. In the multistage design, cluster spacing is a crucial factor in shale gas hydraulic fracturing design. In the case of undersized cluster spacing with too small spacing, the stimulated reservoir volume (SRV) will be affected by major fractures interference where the fractures may overlap each other and decrease the hydraulic fracturing treatment efficiency (Sen et al. 2018). While oversized cluster spacing with too large spacing may lead to a large unstimulated volume in the middle of hydraulic fractures, as a result, the recovery will be impaired. In both cases, hydraulic fracturing would be inefficient. Consequently, optimal design for the cluster spacing is important to improve the SRV and increase the fracturing efficiency (Sharma and Manchanda 2015).

Appropriate spacing is essential to create more fractures in a larger volume and improve well productivity (Pope et al. 2009; Zeng et al. 2016). The industry tends to increase the number of fractures per stage and minimize the fracture spacing in gas shales. It is critical to creating closely spaced multiple fractures to launch commercial oil or gas production rates from a typical shale reservoir with a permeability of 200 to 400 nanodarcies (Waters et al. 2009). However, besides high completion cost and production interference, it is proved that there is a limit for the cluster spacing, and then, the reduction of cluster space will reduce the productivity where some of the perforations do not propagate efficiently. Such inefficient propagation will happen as many fractures propagate simultaneously in a tight space leading to stress shadow, and rising the formation stress will prevent some fractures from propagation (Guo et al. 2015; Miller et al. 2011; Liu et al. 2020; Tan et al. 2022). Simultaneously propagating shows that stress shadow tends to restrict the growth of neighboring fractures and high pumping rates can increase the possibility of making all perforations propagate (Shin and Sharma 2014; Bai et al. 2020; Singh et al. 2020; Yoo et al. 2021).

It is regularly impractical to have fracturing spacing of 1.5 times the fracture height, as, this will extremely limit the

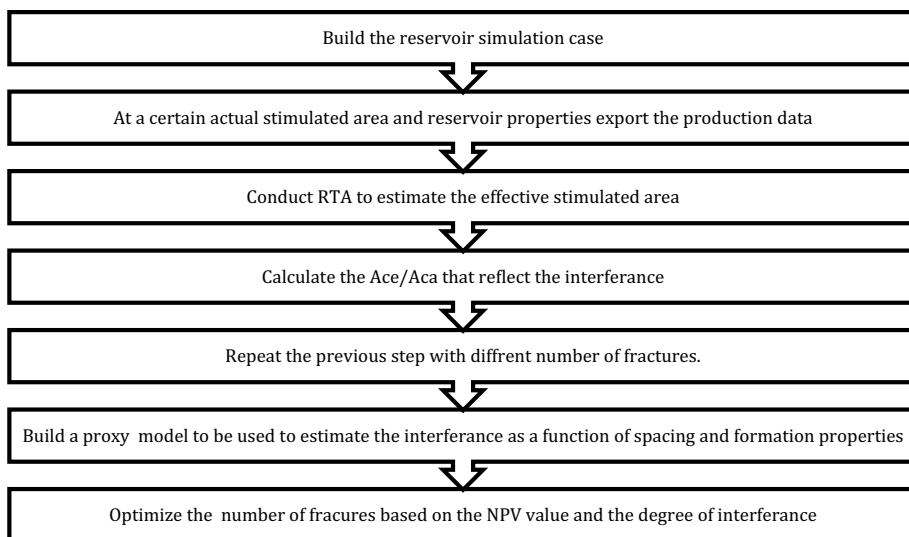
number of created fractures, leading to a small stimulated area and ineffective recovery of a shale-gas reservoir. From a reservoir-engineering viewpoint, it is required to generate more fractures with tighter spacing. Typically, the industry practice applies cluster spacing less than 1.5 times fracture height. For instance, the cluster spacing can be used as 100 ft for a fracture height of 250 ft. In this condition, the effect of stress concentration is not negligible. We need to secure a balance between creating more fractures and mitigating the impact of stress concentration. To realistically optimize fracture design, stress alteration and variable fracture geometry caused by stress concentration must be taken into account (Meyer et al. 2010; Cheng 2012).

Horizontal drilling and multistage hydraulic fracturing are the most common stimulation techniques in shale formations. The economic feasibility and production enhancement of an oil and gas well mainly depend on the efficiency of hydraulically generated fractures. Initially, the cluster spacing tends to be closer to increase the initial production rate. However, a higher initial production rate is at the expense of higher operation and completion costs in addition to operational complexity. In addition to using the fracture propagation model to optimize the cluster spacing, the production or net present value (NPV) should be considered in the optimization process. Short cluster spacing is recommended, but the effective areas for the created fracture will interfere with each other and reduce the completion efficiency at a high cost. On the other hand, the long spacing will lead to thief zones between the fractures and low production rates. Hence, the current study presents a workflow to investigate the degree of fracture interference as a function of cluster spacing and formation properties. To the best of the author knowledge, for the first time, a workflow was built by combining the rate transient analysis with numerical simulation to estimate the degree of fracture interference. In addition, a proxy model was built to predict the degree of interference as a function of completion and formation properties.

Methodology

Figure 1 summarizes the main steps for the workflow to investigate the degree of cluster interference in multistage fractured shale well. Analytical rate transient analysis (RTA) was combined with reservoir numerical simulation to quantify the degree of interference. RTA was used to estimate the effective fracture surface area for hydrocarbon production (A_{Ce}). The ratio between the effective fracture surface area to the actual fracture surface (A_{Ca}) that were used in the numerical simulation represents the degree of interference

Fig. 1 Schematic for the workflow to investigate the fracture interference as a function of formation properties and cluster spacing



between the created fractures. The percentage of interference was defined as $100 * \left(1 - \frac{A_{ce}}{A_{ca}}\right)$.

Numerical simulation process

Reservoir-simulation models were built to simulate gas recovery from shale reservoirs for different cases. One stage was simulated as a unit for the whole horizontal well (Fig. 2). The length of the stage was kept constant to be 250 ft in the different cases. The thickness of the reservoir was selected to be 120 ft. The initial reservoir pressure was set at 5000 psi, while the gas production was constrained at bottom hole pressure of 1000 psi. The gas gravity and the reservoir temperature were set to be 0.65, and 200°F, respectively. A base case was conducted with a formation porosity of 0.065 and permeability of 0.0001 md (100 nd).

The actual fracture surface area (A_a) is calculated using Eq. 1 as follows;

$$A_{Ca} = 4H_f N_f X_f \tag{1}$$

where H_f and X_f are the fracture height and half-length, and N_f is the number of fractures.

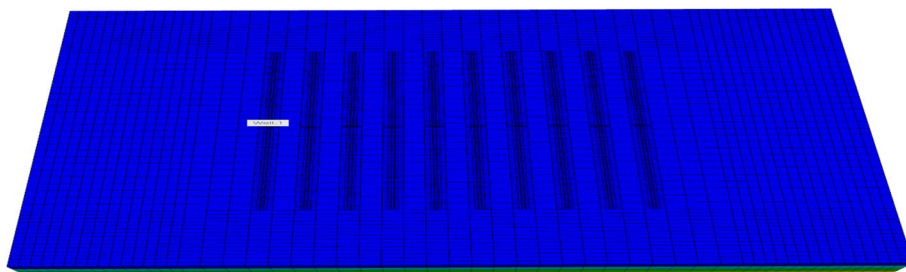
Rate transient analysis process

In RTA for gas wells, bottom-hole pressure, p_{wff} was converted to pseudopressure, $m_{(p_{wff})}$. The pseudopressure difference was then normalized using the gas production rate. The normalized pseudopressure difference and linear superposition time (super- t) were used to plot the RTA for A_c characterization (Nashawi and Malallah 2006). Normalized pseudopressure and linear superposition time were calculated as follows;

$$\text{Normalized pseudopressure difference} = \frac{[m(p_i) - m(p_{wff})]}{q_g} \tag{2}$$

$$m(p) = 2 \int_0^p \frac{p dp}{\mu z} \tag{3}$$

Fig. 2 Schematic for the reservoir model for a hydraulically fractured horizontal well



$$\text{Super} - t = \left[\sum_{j=1}^n \frac{q_j - q_{j-1}}{q_n} \sqrt{t_n - t_{j-1}} \right]^2 \quad (4)$$

where p_i and p_{wf} are the initial reservoir and bottom hole pressures, respectively. μ and z are the gas viscosity and compressibility factors, respectively. n is the time step at which Super - t is calculated, and j is the time step from 0 to n .

With assuming linear flow with infinite fracture conductivity, E1-Banbi and Wattenbarger (1998) solution can be used. Figure 3a shows a diagnostic plot that identifies the linear flow with $1/2$ slope. Figure 3b is a specialized and more definitive plot to identify the linear flow behavior (Ibrahim and Wattenbarger 2005). A straight line was found in the Cartesian plot with a slope (m). $\sqrt{kA_c}$ can be calculated from the line slope (m) (Eq. 5) (E1-Banbi and Wattenbarger 1998).

$$\sqrt{kA_c} = \frac{803.2427}{\sqrt{(\phi\mu c_t)_i}} \left\{ \frac{T}{m} \right\} \quad (5)$$

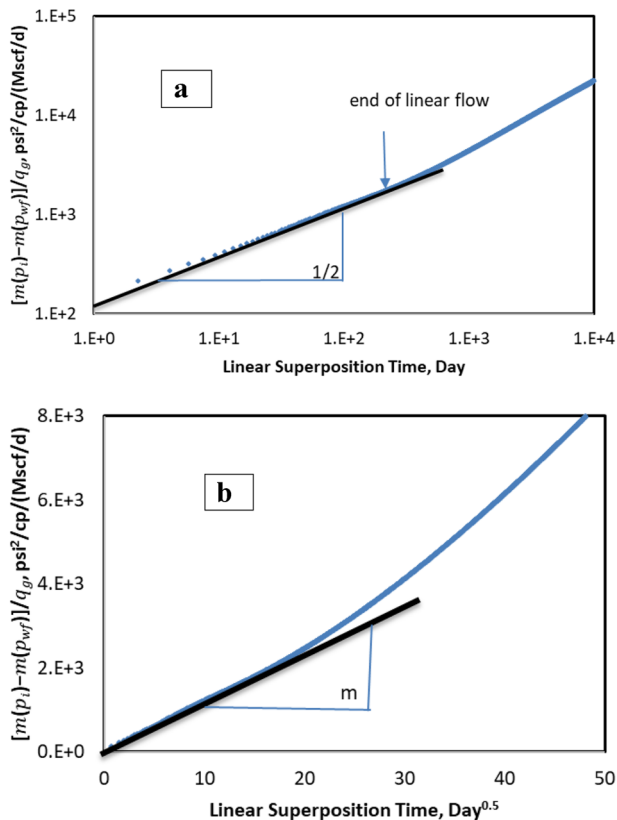


Fig. 3 RTA analysis for gas shale well, **a** diagnostic plot of pseudo-pressure difference divided by rate, $[m(p_i) - m(p_{wf})]/q_g$, versus time, and **b** RTA specialized plot for linear flow regime

where A_c is the total fracture surface area that reflects the effective area for the fluid production, ϕ , μ , c_t are the formation porosity, gas viscosity, and total compressibility, respectively. T is temperature, and k is the formation permeability.

Proxy model using random forest

A proxy model development aims to build a model to predict the fractures interference as a function of cluster spacing and formation properties without the need of running the whole numerical simulation in each case. Different cases were conducted following the flow chart in Fig. 1 to estimate the interference ratio based on the numerical simulation and RTA coupling procedures. A machine learning technique was implemented on this data to develop a proxy model for future prediction of the interference as a function of the formation properties and the cluster spacing.

Random forest (RF) machine learning has been used for many oil and gas applications to predict different parameters based on readily available data. RF is a supervised machine learning technique used for classification and regression problems (Hegde et al. 2015; Yarveicy et al. 2019; Ashraf et al. 2020). RF overcomes the overfitting problems of a single decision tree by combining multiple decision trees. Hence, RF has more accurate predictions, but it is time-consuming as it contains multiple DTs, which, in turn, is slow in providing predictions and it is complex to be interpreted.

RF model was built to predict the interference ratio as a function of formation properties and cluster spacing. The different cases conducted in the previous sections were used to train and test an RF model. The data were randomly spitted into training and testing data sets with a ratio of 70/30. The input features for the model were the formation properties and the cluster spacing, while the target was the interference ratio.

Results and discussion

Fracture interference

In order to examine the percentage of fracture interference, the ratio between the effective fracture surface area (A_{Ce}) and the actual fracture surface area (A_{Ca}) was calculated. For example, the numerical simulator was run using the number of fractures equal to 5 where the cluster spacing is 80 ft. The single fracture half-length was used to be 250 ft. Hence, the actual fracture surface area is calculated from Eq. 1 to be $A_{Ca} = 24 \times 120 \times 5 \times 250 = 6E5$ ft². The numerical simulator was run to predict the production rate

at constant bottom-hole pressure of 1000 psi and a certain formation porosity (0.06) and permeability (0.0005 md). The production and pressure data were analyzed using RTA to estimate the effective fracture surface area. The RTA analysis was conducted as shown in Figs. 2 and 3. The slope of the linear flow regime was found to be $m = 153 \text{ (psi}^2\text{/cp/(Mscf/d)/Day}^{0.5}\text{)}$. This slope was used to calculate the effective surface area ($A_{Ce} = 4.5E5 \text{ ft}^2$). Hence, the ratio was found to be 0.75, that's means there is interference by 25% between the different fractures.

A similar analysis was conducted with changing the number of fractures from 2 to 20 fractures so the cluster spacing varied from 200 to 20 ft. Figure 4 shows the diagnostic plot for each case. All cases showed a linear flow regime first with a 1/2 slope line. The data were then deviated from the straight line to show the end of the linear flow regime and

the beginning of fracture interference. Xiong et al. (2018) showed that the end of linear flowing time depends on the distance between two fractures, permeability, and reservoir fluid property. Once the end of linear flow reaches, the depletion starts and the production rate starts to decline rapidly (Xiong et al. 2018). In this section, the gas viscosity and the stimulated area permeability were set to be constant for the different cases. Hence, the change in the linear flow will be a function of the cluster spacing. At a small number of fractures and long spacing, the linear fracture was dominant and the fracture may not interfere or the interference happens at a late time. While decreasing the fracture spacing, the linear flow regime ends earlier. Figure 5 shows the ratio between the effective to the actual fracture surface areas as a function of the number of fractures (fracture spacing). As the fractures spacing decreases the interference increase, whereas at fracture spacing of 20 ft, the interference was around 50%. In addition, decreasing the cluster spacing to increase the total number of fractures can significantly reduce gas recovery when the cluster spacing is reduced to a small size, where the width growth of fractures is strongly inhibited because of the mechanical interaction and stress shadow effects (Cheng 2012).

Effect of formation properties

To examine the effect of the formation properties on the degree of interference between the fractures, different cases were conducted by changing the formation permeability from 0.00005 to 0.005 md with keeping the formation porosity 0.065 and varying the number of fractures from 1 to 20 fractures per stage. Figure 6A shows the ratio of the effective to the actual fracture surface area (A_{Ce}/A_{Ca}) as a function of the reciprocal

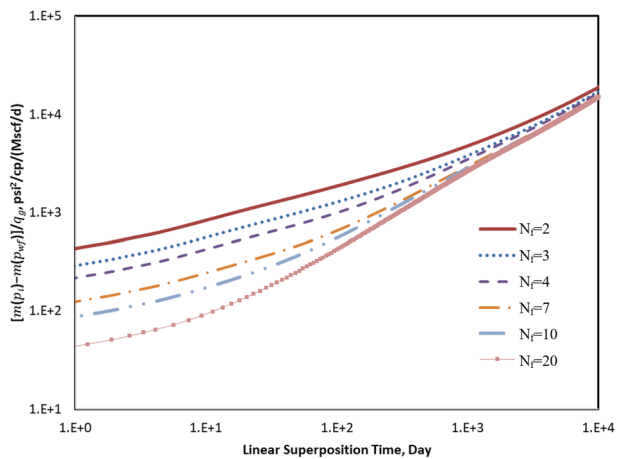


Fig. 4 RTA diagnostic plot of pseudopressure difference divided by rate, $[m(p_i) - m(p_{wf})]/q_g$, versus time

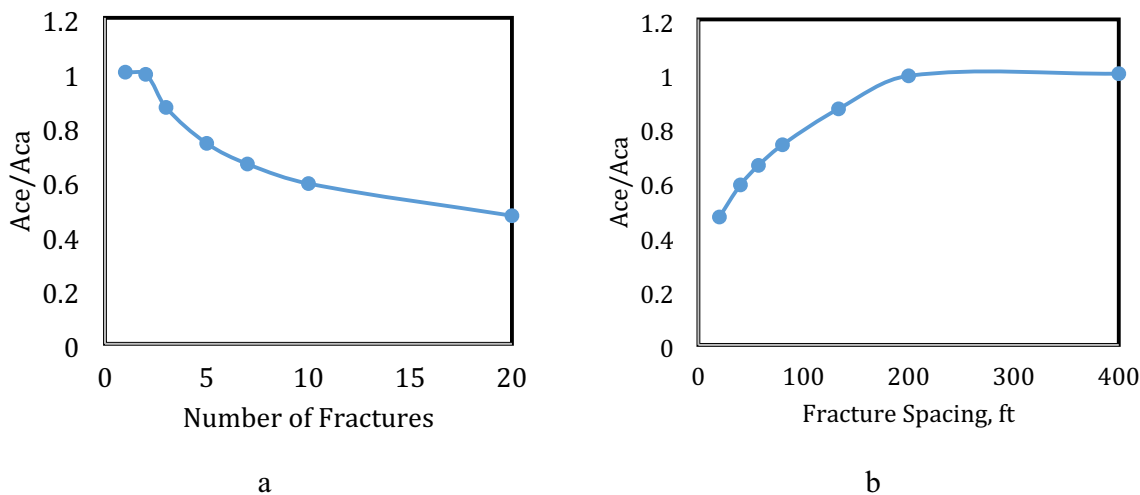


Fig. 5 The effective to the actual fracture surface area ratio as a function of a number of fractures, b fracture spacing

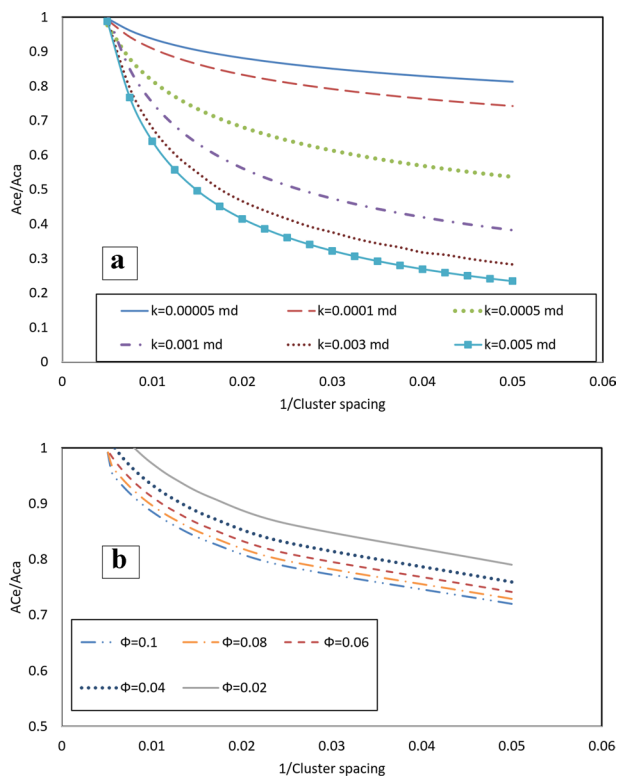


Fig. 6 The effective to the actual fracture surface area ratio as a function of reciprocal fracture spacing at **A** different formation permeabilities, and **B** different formation porosities

of fracture spacing that represents the number of fractures per unit length at different permeability values. At low permeability of 0.00005 md, the fracture interference was very small and becomes more effective at short spacing with 15% interference with a spacing of 20 ft. While at high permeability (0.005 md, for example), the fracture interference was significant even at fracture spacing of 100 ft, the interference was 35%. Xiong (2017) investigated the fracture interference by monitoring the pressure depletion between two fractures with 40 ft spacing after 30-year production at different permeability values from 0.0005 md to 0.00001 md (Fig. 7). He showed that minimal interference was observed at low formation permeability as 0.00001 md and the pressure depletion increases dramatically at formation permeability higher than 0.0001 md which is in agreement with the results from the current study in Fig. 6a.

Similarly, to examine the effect of formation porosity in the interference profile, the analysis was conducted at different porosities from 2 to 10% with formation permeability of 0.0001md (Fig. 6B). The effect of the formation porosity on the interference profile was much less than the permeability effect. With changing the formation porosity from 2 to 10%, the interference increased from 15 to 25%.

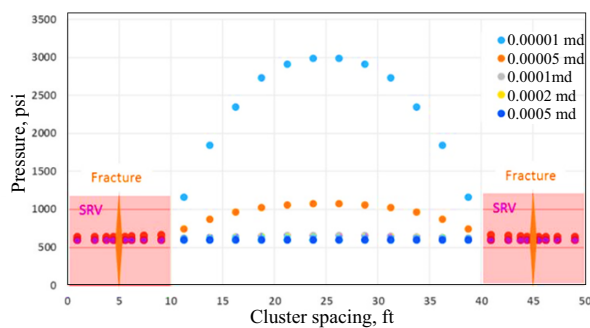


Fig. 7 Effect of formation permeability on pressure depletion between two fractures with spacing of 40 ft, modified after Xiong (2017)

Proxy model development and sensitivity analysis

In this section, a proxy model was developed using random forest (RF) machine learning to predict the interference ratio as a function of formation properties and cluster spacing (Hegde et al. 2015; Yarveicy et al. 2019). The different cases conducted in the previous sections were used to train and test an RF model. The input features for the model were the formation properties and the cluster spacing, while the target was the interference ratio. Figure 8 displays a cross-plot between the actual and the predicted interference ratio using the RF model. Most of the data aligned to the 45-degree line with an R^2 of 0.96, which shows the high accuracy of the developed model and its capabilities to predict the interference ratio.

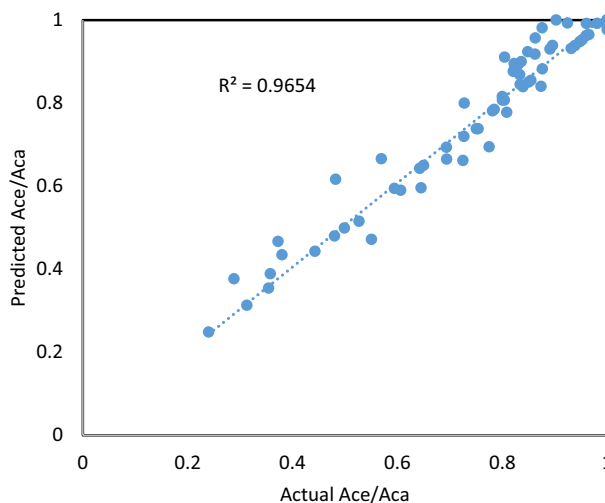


Fig. 8 The actual versus the predicted interference ratio using the random forest model

Table 1 Parameters ranges for the sensitivity analysis

	Minimum	Maximum
Porosity, fraction	0.02	0.1
Permeability, md	5.00E-05	5.00E-03
Spacing, ft	20	200

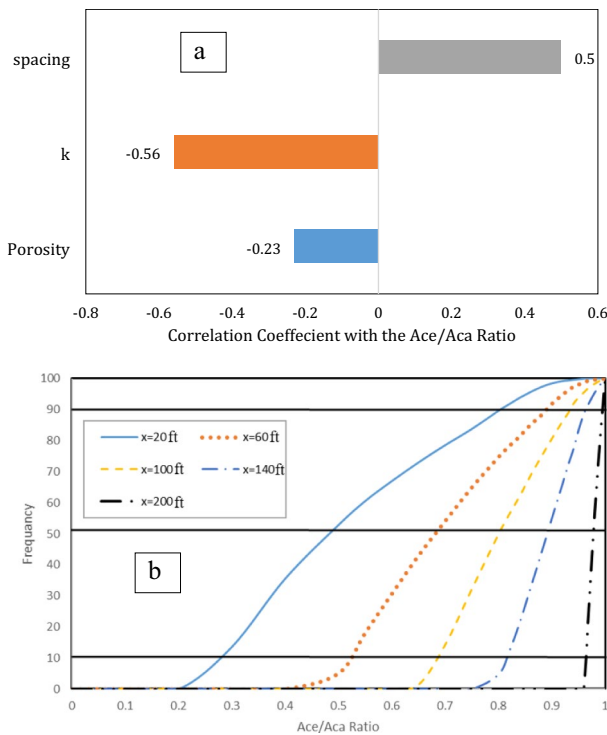


Fig. 9 Sensitivity of formation permeability on the interference, **a** the importance of the different parameters on the interference ratio, and **b** Monte Carlo sensitivity for the input parameters uncertainty

The developed AI model was then used to run a Monte Carlo sensitivity analysis on the effect of formation properties and the fracture spacing on the interference between the fractures. Table 1 shows the ranges for the input parameters for the sensitivity analysis. The porosity ranged from 2 to 10% with the fracture spacing varying from 20 to 200 ft and permeability ranging from 50 to 5000 md. Figure 9a shows the degree of importance for each input parameter on the fracture interference. It showed that the formation permeability is the most effective parameter in the interference

performance followed by the cluster spacing, and finally, the porosity has the lowest correlation coefficient (R) of 0.23 with the A_{Ce}/A_{Ca} ratio. The sign of the correlation coefficient reflects a direct or reverse relationship. For example, R between cluster spacing and the A_{Ce}/A_{Ca} ratio has a positive sign, and hence, as the cluster spacing increases, the A_{Ce}/A_{Ca} ratio increases and the interference between the fracture decreases. While the R for the permeability and the porosity has a $-ve$ sign, so as the porosity and the permeability increase, A_{Ce}/A_{Ca} ratio decreases, which means higher interference.

Monte Carlo analysis was used to investigate the effect of uncertainty of the reservoir parameters on the interference performance at different fracture spacing values (Fig. 9b). With decreasing the fracture spacing, the whole curve shifts to the left and the A_{Ce}/A_{Ca} ratio decreases, which means higher interference. Table 2 summarizes P10, P50, and P90 for the different fracture spacing cases. At fracture spacing of 200 ft, 90% of the wells have A_{Ce}/A_{Ca} a ratio higher than 0.97 that means interference less than 3%. With decreasing the fracture spacing, the A_{Ce}/A_{Ca} ratio decreases, at the spacing of 100 ft, 50% of the wells have A_{Ce}/A_{Ca} a ratio higher than 0.8 that means interference less than 20%. At a tight spacing of 20 ft, 50% of the wells have A_{Ce}/A_{Ca} a ratio higher than 0.53 that means interference less than 47%.

Economic analysis

There are numerous economic analysis approaches in the oil and gas industry including discounted cash flow analysis, cost–benefit incremental method, cost component method, etc. In the current study, discounted cash flow analysis was applied. The analysis is based on calculating the net present value (NPV) from the gas production as a function of capital cost ($CAPEX$), gas price, and interest rate (IRR).

A base case was conducted as the numerical simulator was run to predict the production rate at constant bottom-hole pressure of 1000 psi and a certain formation porosity (0.06) and permeability (0.0005 md). The capital cost was assumed to be \$40,000 per stage, gas price \$3/Mscf, and an interest rate of 20%. Figure 10 shows the NPV results as a

Table 2 A_{Ce}/A_{Ca} ratio probability at different spacings

	Spacing = 200 ft	Spacing = 170 ft	Spacing = 140 ft	Spacing = 100 ft	Spacing = 80 ft	Spacing = 60 ft	Spacing = 20 ft
P10	0.97	0.9	0.83	0.68	0.6	0.53	0.27
P50	0.98	0.95	0.9	0.8	0.75	0.7	0.53
P90	0.995	0.99	0.97	0.94	0.92	0.91	0.81

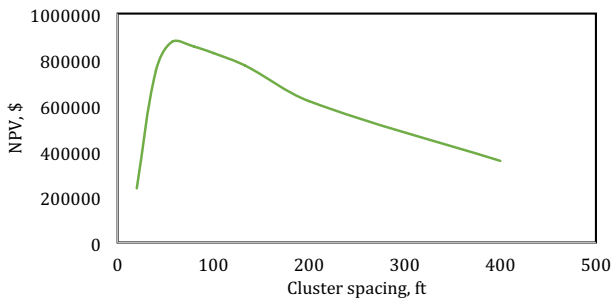


Fig. 10 NPV as a function of fracture spacing for the base case ($k=0.0005$ md, $P_{wf}=1000$ psi, and $\phi = 0.06$)

function of the cluster spacing. At a wider spacing of 400 ft, NPV was estimated to be 0.3MM\$. With increasing the number of fractures by decreasing the spacing, the value of NPV increases until reaches its optimum value at a spacing of 60 ft. As the spacing decreases then the optimum spacing, and hence, the NPV sharply declines. Similar results were observed by Cheng (2012), where the cluster spacing and the number of the cluster had a significant impact on the well’s economics for different four cases.

To examine the effect of permeability on the optimum cluster spacing, the previous analysis was conducted at different formation permeabilities from 0.00005 to 0.005 md (Fig. 11). A similar trend was observed for the NPV versus the fracture spacing. As the permeability increases, the whole curve shifted up and the NPV increases. With increasing the formation permeability increases, the fracture interference increases as shown in Fig. 6, in addition, increasing the permeability already accelerates the production. Hence, as the permeability increases, the optimum cluster spacing

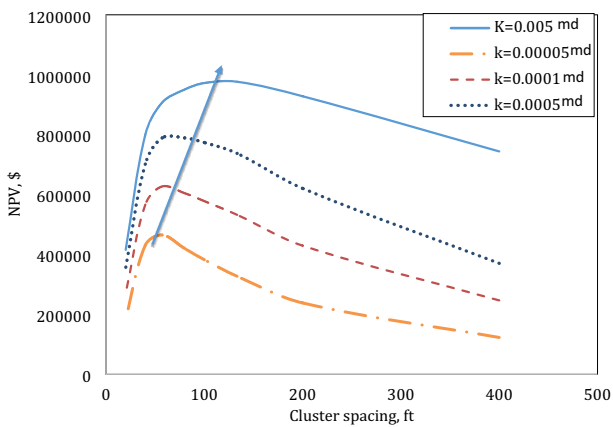


Fig. 11 NPV as a function of fracture spacing for different formation permeabilities

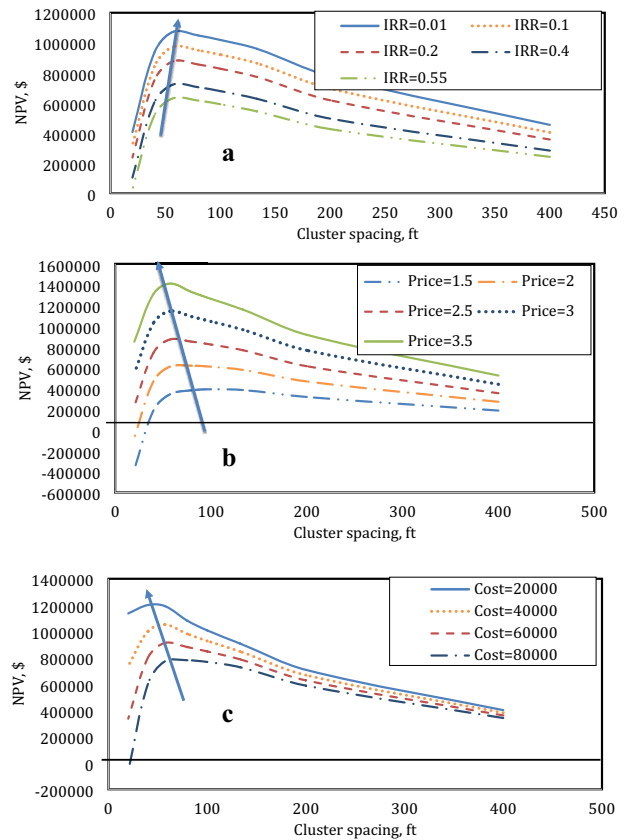


Fig. 12 NPV as a function of fracture spacing for different **A** interest rates, **B** gas prices (\$/Mscf), and **c** capital completion costs (\$/stage)

increases as it changed from 50 to 120 ft when the permeability increases from 0.00005 to 0.005 md.

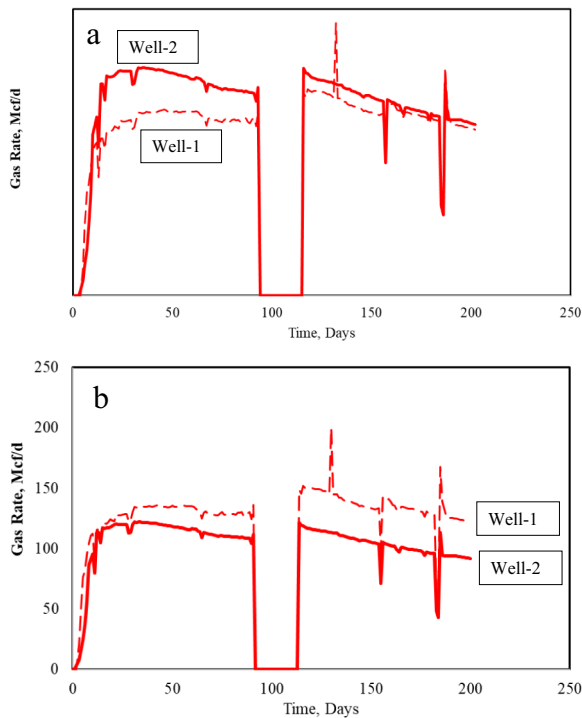
Similarly, the effect of interest rate, gas price, and capital completion cost is investigated as shown in Fig. 12. The interest rate showed a slight effect on the optimum spacing. As the interest rate increased from 0.05 to 0.55, the whole NPV curve shifted down, and optimum spacing becomes tighter from 70 to 40 ft to accelerate the hydrocarbon recovery. In the same way, as the gas prices increased from 1.5 to 3.5 \$/Mscf, the NPV increased and the whole curve shifted up. The optimum spacing decreased from 100 to 40 ft to accelerate the gas production and increase the profit.

As the cluster spacing decreases, the hydrocarbon production accelerated and increases; however, the main drawback is increasing the capital cost with tight spacing. Hence, as the completion cost becomes cheaper and changes from 0.8 to 0.2 MM\$, a tighter spacing is recommended (from 90 to 40 ft) to accelerate the production and improve profitability.

This case study presents the production data for two gas wells in the Barnett shale formation. The two wells were completed with an almost similar design as shown in Table 3. The cluster spacing in well-1 was almost double

Table 3 Completion design for the two wells in the barnett formation

	Well-1	Well-2	Difference %
Water: gal/ft	1715	1,892	10
Sand: lb/ft	1503	1,530	2
Cluster spacing, ft	31	17.4	−44
AVG BPM	67	63	−6
Cost, \$	X	1.3X	30

**Fig. 13** The production data for Well-1 and 2 **a** whole well production, **b** production per stage

the cluster spacing in well-2. For the same lateral length, the completion cost for the second well was 30% higher than the completion cost for well-1. Figure 13 shows the production performance for the two wells. Well-2 with tight fracture spacing showed higher gas production data compared to Well-1, and however, its declining rate was faster. With comparing the production per stage for each well, it shows that Well-1 showed a higher production rate per stage compared to Well-2. Moreover, RTA and PTA analyses were conducted in both wells to estimate the fracture surface area. Even with a lower number of clusters and wider cluster spacing, Well-1 has an almost similar surface area as the one estimated from well-2 (Table 4). That proves that a higher number of fractures with tighter cluster spacing does not always give a higher performance. However, an economic study should be conducted to examine the effect

of production acceleration by increasing the number of fractures versus increasing the capital cost of well completion. Similar case studies were presented by Cote et al. (2019) in Northern Montney, Kakwa/Pipestone Montney, and Pembina West field of the Cardium, where a cluster spacing threshold may have been reached as the progressively reducing the cluster spacing to increase the number of fractures between 2014 and 2018 led to diminished returns. A similar pattern was observed in each case where the production increases with increasing the fracture intensity until a transition point. After the transition point, the production ultimately took a downturn despite continued increases in fracture intensity (Cote et al. 2019).

Conclusion

The current study presents an integrated workflow to examine the effect of fracture interference on well performance. Rate transient analysis was combined with numerical simulation to quantify the degree of fracture interference based on the formation properties and cluster spacing. The main conclusions are summarized as follows:

1. The higher stage number and tighter cluster spacing will have high cluster interference with low effective to actual fracture surface area ratio.
2. The formation permeability is the dominant parameter in fracture interface behavior.
3. The porosity correlated with effective to actual fracture surface area ratio by R -value of -0.23 compared to -0.56 in case of formation permeability.
4. A proxy model was built to predict the degree of fracture interference as a function of formation properties and the cluster spacing with R^2 of 0.96 between the actual and the predicted values.
5. Based on the uncertainty analysis, regardless of the formation properties, at a spacing of 100 ft, 50% of the wells have means interference higher than 20%. While at a tight spacing of 20 ft, 90% of the wells have interference higher than 20%.
6. From the economic study, spacing of 60 ft was found to be the optimum spacing based on the formation properties, capital cost, and gas price. As the interest rate gas

Table 4 PTA analysis results for the two wells

VR Model results	PTA analysis	
	Well-1	Well-2
Wellbore storage, bbl/psi	0.0085127	0.0197008
Skin	0.141931	0.065
A_c , acre = $4 N_f X_f h_f$, Acr	67	69

prices increased, or a low capital costs, the optimum completion tends to be with tighter spacing to accelerate the production.

7. Based on the Barnett wells case study, regardless of the number of fracturing stages, for the same lateral length and the same injected frac proppant, the cumulative gas production will be the same.
8. The well with higher stage number and tighter cluster spacing will drain the production area faster with a high initial production rate.
9. The well with low number of stages will drain the same area but for a longer time and lower initial production rate.

Funding No External fund for this research and the authors would like to thank KFUPM for giving permission to publish this work.

Declarations

Conflict of interest The authors declare that they have no known competing financial interests or personal relationships that could have appeared to influence the work reported in this paper.

Open Access This article is licensed under a Creative Commons Attribution 4.0 International License, which permits use, sharing, adaptation, distribution and reproduction in any medium or format, as long as you give appropriate credit to the original author(s) and the source, provide a link to the Creative Commons licence, and indicate if changes were made. The images or other third party material in this article are included in the article's Creative Commons licence, unless indicated otherwise in a credit line to the material. If material is not included in the article's Creative Commons licence and your intended use is not permitted by statutory regulation or exceeds the permitted use, you will need to obtain permission directly from the copyright holder. To view a copy of this licence, visit <http://creativecommons.org/licenses/by/4.0/>.

References

- Al-Muntasheri GA, Nasr-El-Din HA, Khalid S, Zitha PLJ (2009) A Study of polyacrylamide-based gels crosslinked with polyethyleneimine. *SPE J* 14(02):245–251. <https://doi.org/10.2118/105925-PA>
- Ashraf U, Zhang H, Anees A, Nasir Mangi H, Ali M, Ullah Z, Zhang X (2020) Application of unconventional seismic attributes and unsupervised machine learning for the identification of fault and fracture network. *Appl Sci* 10(11):3864
- Bai Q, Liu Z, Zhang C, Wang F (2020) Geometry nature of hydraulic fracture propagation from oriented perforations and implications for directional hydraulic fracturing. *Comput Geotech* 125:103682. <https://doi.org/10.1016/J.COMPGEO.2020.103682>
- Beckwith R (2011) Shale gas: promising prospects worldwide. *J Pet Technol* 63(07):37–40. <https://doi.org/10.2118/0711-0037-JPT>
- Cheng Y (2012) Impacts of the number of perforation clusters and cluster spacing on production performance of horizontal shale-gas wells. *SPE Reserv Eval Eng* 15(01):31–40. <https://doi.org/10.2118/138843-PA>
- Cote A, Cameron N, Grunberg D (2019) When is there too much fracture intensity?. In: Paper presented at the SPE annual technical conference and exhibition, Calgary, Alberta, Canada, SPE-195895-MS. <https://doi.org/10.2118/195895-MS>
- E1-Banbi AH, Wattenbarger RA (1998) Analysis of linear flow in gas well production. In: SPE gas technology symposium, Calgary, Alberta, Canada, Paper Number SPE-39972-MS, pp 1–18. <https://doi.org/10.2118/39972-MS>
- Emrani AS, Ibrahim AF, Nasr-El-Din HA (2017) Mobility control using nanoparticle-stabilized CO₂ foam as a hydraulic fracturing fluid. In: SPE europepec featured at 79th EAGE conference and exhibition, Paris, France, Paper Number SPE-185863-MS. <https://doi.org/10.2118/185863-MS>
- Guo J, Lu Q, Zhu H, Wang Y, Ma L (2015) Perforating cluster space optimization method of horizontal well multi-stage fracturing in extremely thick unconventional gas reservoir. *J Nat Gas Sci Eng* 26:1648–1662. <https://doi.org/10.1016/J.JNGSE.2015.02.014>
- Hegde C, Wallace S, Gray K (2015) Using trees, bagging, and random forests to predict rate of penetration during drilling. In: Paper presented at the SPE middle east intelligent oil and gas conference and exhibition, Abu Dhabi, UAE, September 2015
- Ibrahim AF, Nasr-El-Din HA, Rabie A, Lin G, Zhou J, Qu Q (2018) A new friction-reducing agent for slickwater-fracturing treatments. *SPE Prod Oper* 33(03):583–595. <https://doi.org/10.2118/180245-PA>
- Ibrahim M, Wattenbarger RA (2005) Analysis of rate dependence in transient linear flow in tight gas wells. In: Canadian international petroleum conference 2005, CIPC 2005, Calgary, Alberta, Paper Number PETSOC-2005-057. <https://doi.org/10.2118/2005-057>
- Jiang R, Zhao L, Xu A, Ashraf U, Yin J, Song H, Anees A (2021) Sweet spots prediction through fracture genesis using multi-scale geological and geophysical data in the karst reservoirs of cambrian longwangmiao carbonate formation moxi-gaoshiti area in sichuan basin South China. *J Pet Explor Prod Technol*. <https://doi.org/10.1007/s13202-021-01390-0>
- King GE (2010) Thirty years of gas-shale fracturing: what have we learned? *J Pet Technol* 62(11):88–90. <https://doi.org/10.2118/1110-0088-JPT>
- Kolawole O, Esmailpour S, Hunky R, Saleh L, Ali-Alhaj HK, Marghani M (2019) Optimization of hydraulic fracturing design in unconventional formations: impact of treatment parameters. In: Society of petroleum engineers-SPE kuwait oil and gas show and conference 2019, KOGS 2019. <https://doi.org/10.2118/198031-MS>
- Liu X, Rasouli V, Guo T, Qu Z, Sun Y, Damjanac B (2020) Numerical simulation of stress shadow in multiple cluster hydraulic fracturing in horizontal wells based on lattice modelling. *Eng Fract Mech* 238:107278
- Meyer BR, Bazan LW, Jacot RH, Lattibeaudiere MG (2010) Optimization of multiple transverse hydraulic fractures in horizontal wellbores. In: SPE unconventional gas conference 2010, pittsburgh, pennsylvania, USA, Paper Number SPE-131732-MS, pp 58–94. <https://doi.org/10.2118/131732-MS>
- Miller C, Waters G, Rylander E (2011) Evaluation of production log data from horizontal wells drilled in organic shales. In: Society of petroleum engineers-SPE americas unconventional gas conference 2011, UGC 2011, pp 623–645. <https://doi.org/10.2118/144326-MS>
- Nashawi IS, Malallah A (2006) Rate derivative analysis of oil wells intercepted by finite conductivity hydraulic fracture. In: Canadian international petroleum conference, Calgary, Alberta, Paper Number PETSOC-2006-121. <https://doi.org/10.2118/2006-121>
- Pope C, Peters B, Benton T, Palisch T (2009) Haynesville shale-one operator's approach to well completions in this evolving play. In: Proceedings-SPE annual technical conference and exhibition, 7, pp 4339–4350. <https://doi.org/10.2118/125079-MS>

- Seale R, Donaldson J, Athans J (2006) Multistage fracturing system: improving operational efficiency and production. In: SPE eastern regional meeting, Canton, Ohio, USA, Paper Number SPE-104557-MS 2006, pp 218–225. <https://doi.org/10.2118/104557-MS>
- Sen V, Min, KS, Ji L, Sullivan R (2018) Completions and well spacing optimization by dynamic *SRV* modeling for multi-stage hydraulic fracturing. In: Proceedings-SPE annual technical conference and exhibition, pp 24–26. <https://doi.org/10.2118/191571-MS>
- Sharma MM, Manchanda R (2015) The role of induced un-propped (iu) fractures in unconventional oil and gas wells. In: SPE annual technical conference and exhibition, Houston, Texas, USA, Paper Number SPE-174946-MS 2015-Janua, pp 3039–3052. <https://doi.org/10.2118/174946-MS>
- Shin DH, Sharma MM (2014) Factors controlling the simultaneous propagation of multiple competing fractures in a horizontal well. In: SPE Hydraulic fracturing technology conference 2014, The Woodlands, Texas, USA, Paper Number SPE-168599-MS, pp 269–288. <https://doi.org/10.2118/168599-MS>
- Singh A, Xu S, Zoback M, McClure M (2019) Integrated analysis of the coupling between geomechanics and operational parameters to optimize hydraulic fracture propagation and proppant distribution. In: Society of petroleum engineers-SPE hydraulic fracturing technology conference and exhibition 2019, HFTC 2019, pp 5–7. <https://doi.org/10.2118/194323-MS>
- Singh A, Zoback M, McClure M (2020) Optimization of multi-stage hydraulic fracturing in unconventional reservoirs in the context of stress variations with depth. In: Proceedings-SPE annual technical conference and exhibition, p 201739. <https://doi.org/10.2118/201739-MS>
- Tan P, Jin Y, Fu S, Chen Z (2022) Experimental investigation on fracture growth for integrated hydraulic fracturing in multiple gas bearing formations. SSRN Electron J. <https://doi.org/10.2139/SSRN.4055304>
- Ullah J, Luo M, Ashraf U, Pan H, Anees A, Li D, Ali J (2022) Evaluation of the geothermal parameters to decipher the thermal structure of the upper crust of the longmenshan fault zone derived from borehole data. *Geothermics* 98:102268
- Waters G, Dean B, Downie R, Kerrihard K, Austbo L, McPherson B (2009) Simultaneous hydraulic fracturing of adjacent horizontal wells in the woodford shale. In: SPE hydraulic fracturing technology conference 2009, The Woodlands, Texas, Paper Number SPE-119635-MS, pp 694–715. <https://doi.org/10.2118/119635-MS>
- Wiley C, Barree B, Eberhard M, Lantz T (2004) Improved horizontal well stimulations in the bakken formation, Williston Basin, Montana. In: SPE annual technical conference and exhibition, Houston, Texas, Paper Number SPE-90697-MS, pp 3559–3568
- Xiong H, Wu W, Goa S (2018) Optimizing well completion design and well spacing with integration of advanced multi-stage fracture modeling & reservoir simulation - a permian basin case study. In: Society of petroleum engineers-SPE hydraulic fracturing technology conference and exhibition 2018, HFTC 2018, 2, p 189855. <https://doi.org/10.2118/189855-MS>
- Xiong H (2017) Optimizing cluster or fracture spacing—an overview. In: SPE the way ahead. <https://jpt.spe.org/twa/optimizing-cluster-or-fracture-spacing-overview>
- Yarveicy H, Saghafi H, Ghiasi MM, Mohammadi AH (2019) Decision tree-based modeling of CO₂ equilibrium absorption in different aqueous solutions of absorbents. *Environ Prog Sustain Energy* 38(s1):S441–S448. <https://doi.org/10.1002/ep.13128>
- Yoo J, Park H, Wang J, Sung W (2021) Analysis of hydraulic fracture geometry by considering stress shadow effect during multi-stage hydraulic fracturing in shale formation. *J Korean Inst Gas* 25(1):20–29. <https://doi.org/10.7842/KIGAS.2021.25.1.20>
- Zeng Y, Chen Z, Bian X (2016) Breakthrough in staged fracturing technology for deep shale gas reservoirs in SE Sichuan Basin and its implications. *Nat Gas Ind B* 3(1):45–51. <https://doi.org/10.1016/J.NGIB.2016.02.005>

Publisher's Note Springer Nature remains neutral with regard to jurisdictional claims in published maps and institutional affiliations.